Response Time Distributions in Partially-Coherent Quantum Walk Models for Simple Decision Tasks

Ian G. Fuss (ifuss@eleceng.adelaide.edu.au)
School of Electrical and Electronic Engineering, University of Adelaide, SA 5005, Australia

Daniel J. Navarro (daniel.navarro@adelaide.edu.au)
School of Psychology, University of Adelaide, SA 5005, Australia

Abstract

Psychological models for two-choice decision tasks typically model the probability that a particular response is made at time t via the first-passage time to an absorbing boundary for some stochastic process. In contrast to the most commonly used models which use classical random walks for the underlying process, a recent paper by Busemeyer, Wang, and Townsend (2006) proposed that quantum walks may provide an interesting alternative. In this paper, we extend this work by introducing a class of *partially-coherent quantum walk models* that can be applied to human two-choice tasks. The models trace out a path from quantum to classical models, preserving some of the desirable features of both. We discuss the properties of these models, and the implications for modeling simple decisions.

Keywords: decisions, response time, quantum mechanics

The hypothesis that human induction and decision-making can exploit quantum mechanical phenomena is one that has a great deal of intuitive appeal. Perhaps the currently most famous version of this hypothesis is Penrose's (Penrose, 1989) suggestion that mathematical insight relies on quantum mechanical effects. Although a number of aspects of that specific version of the hypothesis are controversial (e.g., Litt, Eliasmith, Kroon, Weinstein, & Thagard, 2006; Hameroff, 2007) there is a certain face validity to the general idea. In particular, one of the most basic findings from quantum computing is that it is possible to exploit the parallelism inherent in quantum mechanics to speed up a number of computational problems (Shor, 1994, 1997; Grover, 1997). Since human decision processes unfold over time, it is plausible to suggest that an evolutionary advantage would accrue to decision-makers that can make effective use of quantum mechanical effects. Of course, many questions need to be answered before we can determine with any confidence whether or not this advantage has in fact been achieved by living organisms. Indeed, at least four important scientific perspectives have significant bearing on these questions, namely psychology, biology, computer science and physics (see Litt et al., 2006, for instance). This paper is concerned primarily with psychological topics but relies on insights from the other three fields.

From the psychological perspective, one of the main issues with which we must be concerned is the construction of formal models that make predictions about human behavior. That is, if the brain can make use of quantum phenomena in its processing, or (in a weaker formulation) obeys dynamical laws that reflect the mathematical structure of quantum mechanics, what patterns would one expect to observe in human behavior? In this paper, we adopt the weaker "functionalist" perspective, and consider psychological models that use quantum mechanical principles. The stronger claim, that human information processing genuinely makes use of quantum physical phenomena, is beyond the scope of this paper.

In a pioneering paper, Busemeyer et al. (2006) explored the possibility of a formal characterization of human decision making processes based on quantum mechanical principles. Their model was constructed as a quantum mechanical analog of a standard random walk model (e.g., Stone, 1960) for human decisions and decision latencies. They found that this quantum mechanical model could reproduce some of the basic findings in the literature on human decision-making. In this paper we extend this work in two respects. Firstly, we consider a more general quantum walk that has its origins in computer science and physics (Aharonov, Davidovich, & Zagury, 1993; Meyer, 1996). We cast this quantum walk into a linear systems framework (Fuss, White, Sherman, & Naguleswaran, 2007) that allows us to demonstrate the similarities to and differences from a classical random walk. Secondly, we employ a density matrix formalization of the walk, allowing us to extend the quantum walk framework to accommodate the influence of noise on the evolution of the walk. This second aspect produces *partially-coherent quantum walk models*, which subsume both classical and quantum walks as special cases. When high levels of noise are injected into the walk, the quantum state decoheres completely, and the model reduces to a Bernoulli random walk. When the noise levels are set to zero, we obtain a pure quantum walk model. As a result, we arrive at a model for human decision making that allows us to infer the extent to which quantum behaviour is manifest.

The structure of this paper is as follows. In the first section, we introduce two walk processes, one classical and one quantum, and discuss their interpretations as linear systems. We then discuss the use of absorbing boundaries as psychological decision criteria, and the calculation of the first passage time distributions for both processes. Having constructed these special cases, we then introduce the more general partially-coherent walks, and discuss two plausible noise processes. Finally, we provide a brief discussion of the behavior of the first passage time distributions for partially-coherent walks, as a function of the amount and type of noise involved.

Sequential Sampling Models, Classical and Quantum

Our approach, like that of Busemeyer et al. (2006), is based on a general class of sequential sampling models commonly used to describe human evidence-accrual and

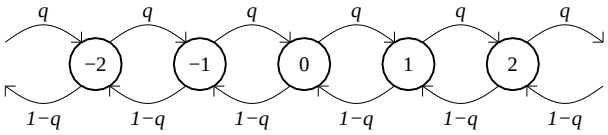

Figure 1: The transition diagram for a Bernoulli random walk. Each node corresponds to a possible location x for the walk, and each link is labelled by the amount of probability mass that transfers between locations at each time point.

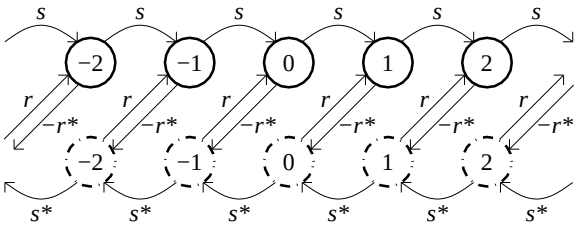

Figure 2: The transition diagram for a two-state quantum walk. Each node corresponds to one element of the state vector, with the top row corresponding to the right-handed elements, and the bottom row to the left-handed elements. Each node is labelled with its location x. The coefficients r, r^*, s and s^* refer to the amount of probability amplitude that transfers between different elements (in this illustration, we set $k = 0$ for simplicity).

decision-making (e.g., Ratcliff & Smith, 2004). The central assumption of such models is that the environment provides people only with noisy stimulus representations, and so to make accurate decisions people draw successive samples from this representation until some *decision threshold* is reached. This class of models (see, e.g., Ratcliff, 1978; Vickers, 1979; Smith & van Zandt, 2000) draws heavily from sequential analysis (Wald, 1947) and stochastic processes (Smith, 2000), and is at present the best formal framework available for modeling decision accuracy, latency, and subjective confidence in simple decision tasks.

Bernoulli Random Walks

The simplest kind of sequential sampling model relies on Bernoulli sampling in discrete time. At each time point, the observer accrues a single piece of evidence drawn from a Bernoulli distribution: with probability q, the evidence favors response A, and with probability $1 - q$ it favors response B. The observer draws samples until some decision threshold is reached; typically, when the number of samples favoring one option exceeds the number of samples favoring the other option by some fixed amount. A procedure of this kind defines a discrete random walk on the line, taking a step up with probability q and a step down with probability $1 - q$, and the decision thresholds that terminate this process act as *absorbing boundaries* (e.g., Smith, 2000). Commonly, one applies a variant of the so-called "assumption of small steps" (see Luce 1986) and takes the limit to a continuous Wiener diffusion model (Feller, 1968; Ratcliff, 1978). For conceptual simplicity, however, we retain the original Bernoulli model.

Formally, in the discrete Bernoulli random walk, we consider the evolution of the probability distribution $p(x, t) \in \mathbb{R}$ for discrete times $t \geq 0$, and possible locations $x \in \mathbb{Z}$, from an initial distribution over locations $p(x, 0)$. The dynamics of this walk evolve according to the linear difference equation

$$p(x, t + 1) = qp(x - 1, t) + (1 - q)p(x + 1, t), \quad (1)$$

where $q \in [0, 1]$. The transition diagram for this difference equation is given in Figure 1, and illustrates how the probability mass is transferred between successive time points. Since it is a linear system, Equation 1 can be written in matrix form,

$$\boldsymbol{p}(t + 1) = \mathbf{M}\boldsymbol{p}(t), \quad (2)$$

where the transpose of the probability state vector is

$$\begin{aligned} \boldsymbol{p}^{\mathsf{T}}(t) \quad = \quad & (\ldots p(-2, t), p(-1, t), p(0, t), \\ & p(1, t), p(2, t), \ldots), \end{aligned} \quad (3)$$

and the one-step time evolution matrix is

$$\mathbf{M} = \begin{bmatrix} \cdot & \cdot & \cdot & \cdot & \cdot & \cdot \\ \cdot & 0 & 1-q & 0 & 0 & \cdot \\ \cdot & q & 0 & 1-q & 0 & \cdot \\ \cdot & 0 & q & 0 & 1-q & \cdot \\ \cdot & 0 & 0 & q & 0 & \cdot \\ \cdot & \cdot & \cdot & \cdot & \cdot & \cdot \end{bmatrix}. \quad (4)$$

Note that the columns of $\mathbf{M}$ sum to 1, preserving the isometry constraint (that probabilities sum to 1 at all times).

Although it is somewhat unnecessary for Bernoulli walks, since analytic expressions exist for most of their interesting psychological properties (Feller, 1968), this kind of matrix formulation is very useful in general. As discussed by Diederich and Busemeyer (2003), adopting simple matrix representations for evidence accrual processes serves a useful pragmatic goal, insofar as it simplifies the subsequent calculation of model predictions in those cases where analytic expressions do not exist.

Quantum Walks

The Bernoulli random walk is a classical model: it traces out a single path on the line. However, in a quantum system there is an inherent parallelism, insofar as (in the absence of measurement) the evidence-accrual process now traces out multiple paths simultaneously. Consequently, the variance of a quantum walk increases quadratically with time in contrast to a linear increase of the variance for a Bernoulli random walk. Hence we would expect a quantum decision maker to make decisions considerably faster than the corresponding classical decision maker. In this section, we describe the basic quantum walk model.

Quantum walks differ from classical ones in two main respects: firstly, although the dynamics are still linear, they are described with respect to probability amplitudes (complex numbers whose squared absolute values sum to 1), not probabilities (real numbers that sum to 1); and secondly in order to preserve isometry on the probabilities, the operator must be unitary. Unitarity imposes strong constraints on the kinds of dynamics that may be considered, and as a consequence, quantum walks in which the particle has only a *location* $x \in \mathbb{Z}$ are extremely uninteresting. Typically, this is addressed by allowing the particle to have a *chirality* (left or right) as well as a location. The state of the walk at time t is then described by the spinor

$$\boldsymbol{\psi}(x, t) = \begin{pmatrix} \psi_R(x, t) \\ \psi_L(x, t) \end{pmatrix}, \quad (5)$$

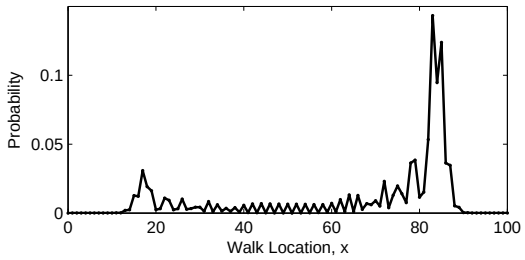

Figure 3: The distribution of a Hadamard walk, measured at $t = 50$. The initial state of the walk places probability amplitude $1/2$ for both chiralities at the location $x = 50$, and amplitude $1/2\sqrt{2}$ at both chiralities for $x = 49$ and $x = 51$ (essentially an analog of the Bernoulli case with probability 1/2 in the middle location, and 1/4 on either side).

where $\psi_R(x,t) \in \mathbb{C}$ is a complex-valued scalar that describes the probability amplitude in state x with right-chirality at time t. A natural analog of the Bernoulli walk for this system involves some probability amplitude moving from the location x to the locations $x+1$ or $x-1$, but with the chirality changing as well. More precisely, the dynamics of the state evolve according to the difference equations (Aharonov et al., 1993; Meyer, 1996)

$$\begin{aligned} \psi_R(x,t+1) &= e^{ik}\left[s\psi_R(x-1,t) + r\psi_L(x-1,t)\right] \\ \psi_L(x,t+1) &= e^{ik}\left[-r^*\psi_R(x+1,t) + s^*\psi_L(x+1,t)\right], \end{aligned} \tag{6}$$

where $|r|^2 + |s|^2 = 1$, s^* is the complex conjugate of s, and $k \in \mathbb{R}$. The structure of this walk is illustrated by the transition diagram in Figure 2, which describes the one-step evolution for the probability amplitudes, in the case where $k = 0$. Notice that the coefficient s controls the probability amplitude that stays in the same chirality, with amplitudes in the left chirality consistently moving leftward (i.e., x decreases), and amplitudes in the right chirality moving right (x increases). The coefficient r controls the "reversal" of the chirality from left to right and vice versa. In order to illustrate the basic characteristics of this kind of quantum walk, Figure 3 shows what happens when a so-called "Hadamard walk" (where $e^{ik} = i$ and $s = r = i/\sqrt{2}$) is evolved for 50 time steps and then measured.

Decisions and First Passage Times

The development so far describes an evidence-accrual process that (be it classical or quantum mechanical) evolves without constraint on $x \in \mathbb{Z}$. Psychologically, however, since x is interpreted as an evidence value, and time is of the essence to the decision-maker, it is generally assumed that once x hits either 0 or a, the evidence-accrual terminates and a decision is made. Accordingly, both 0 or a act as absorbing boundaries, and the decision latency is described by the *first passage time distribution* to the boundaries.

Bernoulli Random Walks

Not surprisingly, the classical case is straightforward: in order to calculate the first passage times to absorbing boundaries at $x = 0$ and $x = a$ we modify the Bernoulli random walk to have the transition diagram shown in Figure 4. The nodes at $x = 0$ and $x = a$ will thus contain the cumulative distribution of absorbed particles at a given time. Since we are interested in first passage times it is convenient to relax the requirement that $\mathbf{M}$ produce an isometry by dropping the self-transitions on the end nodes. They will then contain the first passage time probability for that time. If we choose $a = 4$ then the one step time evolution matrix is

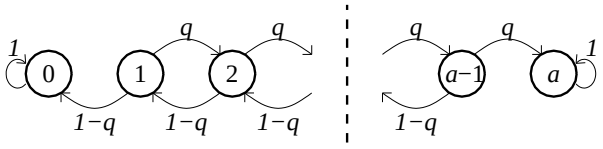

Figure 4: The transition diagram for an absorbing boundary random walk. The structure differs from that in Figure 1 only in that the states $x = 0$ and $x = 1$ do not send probability mass to other states: instead, all probability mass is preserved in the self-transition links at each end of the diagram.

$$\mathbf{M} = \begin{bmatrix} 0 & 1-q & 0 & 0 & 0 \\ 0 & 0 & 1-q & 0 & 0 \\ 0 & q & 0 & 1-q & 0 \\ 0 & 0 & q & 0 & 0 \\ 0 & 0 & 0 & q & 0 \end{bmatrix}. \tag{7}$$

The model is completed by a choice of the initial state such as $\boldsymbol{p}^{\mathsf{T}}(0) = (0,0,1,0,0)$. Hence, $p(0,t)$ is the first passage time distribution for the $x = 0$ boundary and $p(4,t)$ is the first passage time distribution for the $x = 4$ boundary.

Quantum Walks

The absorbing boundary problem for quantum walks is a little more subtle. We define the projection operators

$$\mathbf{P}_e = |x \le 0\rangle\langle x \le 0| \tag{8}$$
$$\mathbf{P}_f = |0 < x < a\rangle\langle 0 < x < a| \tag{9}$$
$$\mathbf{P}_c = |a \le x\rangle\langle a \le x|, \tag{10}$$

where $\mathbf{P}_e$ projects from the Hilbert space containing the spinors $\boldsymbol{\psi}$ onto its subspace with support $[-\infty, 0]$ and similarly $\mathbf{P}_f$ projects onto the subspace with support $(0, a)$ and $\mathbf{P}_c$ projects onto the subspace with support $[a, \infty]$. We consider the problem where at each time t we make partial measurements of the quantum walk with the operators $\mathbf{P}_e$ and $\mathbf{P}_c$. This effectively modifies the time evolution process described by the transition diagram in Figure 2 to one described by transition diagrams such as that in Figure 5, where we have chosen the case where $a = 4$ for simplicity.

We can write a matrix equation

$$\boldsymbol{\psi}_{4c}(t+1) = \mathbf{U}_{4c}\boldsymbol{\psi}_{4c}(t) \tag{11}$$

for the operations described by this transition diagram, where

$$\begin{aligned} \boldsymbol{\psi}_{4c}^{\mathsf{T}}(t) = (&\psi_R(0,t), \psi_L(0,t), \psi_R(1,t), \psi_L(1,t), \\ &\psi_R(2,t), \psi_L(2,t), \psi_R(3,t), \psi_L(3,t), \\ &\psi_R(4,t), \psi_L(4,t)), \end{aligned} \tag{12}$$

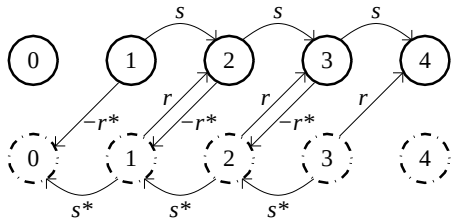

Figure 5: The transition diagram for a quantum walk with absorbing boundaries, in which we set $a = 4$, and remove the self-transition edges. In all other respects, the transition structure mimics the one in Figure 2.

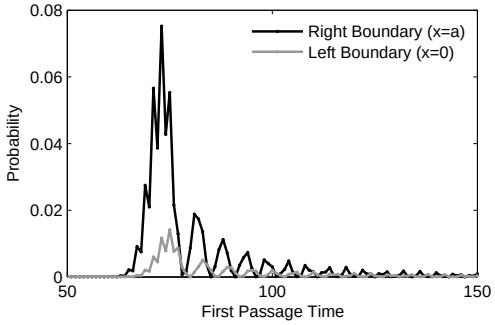

Figure 6: First passage times to the two boundaries (with $a = 100$) for the Hadamard walk in Figure 3. The extreme multimodality of these distributions is not generally a characteristic of empirical RT distributions (e.g. Ratcliff & Smith, 2004).

and the one-step time evolution matrix is

$$\mathbf{U}_{4c} = e^{ik} \begin{bmatrix} 0 & 0 & 0 & 0 & 0 & 0 & 0 & 0 & 0 & 0 \\ 0 & 0 & -r^* & s^* & 0 & 0 & 0 & 0 & 0 & 0 \\ 0 & 0 & 0 & 0 & 0 & 0 & 0 & 0 & 0 & 0 \\ 0 & 0 & 0 & 0 & -r^* & s^* & 0 & 0 & 0 & 0 \\ 0 & 0 & s & r & 0 & 0 & 0 & 0 & 0 & 0 \\ 0 & 0 & 0 & 0 & 0 & 0 & -r^* & s^* & 0 & 0 \\ 0 & 0 & 0 & 0 & s & r & 0 & 0 & 0 & 0 \\ 0 & 0 & 0 & 0 & 0 & 0 & 0 & 0 & 0 & 0 \\ 0 & 0 & 0 & 0 & 0 & 0 & s & r & 0 & 0 \\ 0 & 0 & 0 & 0 & 0 & 0 & 0 & 0 & 0 & 0 \end{bmatrix}. \quad (13)$$

We complete the matrix specification by defining an initial state $\boldsymbol{\psi}_{4c}^{\mathsf{T}}(0)$. The first passage time distributions to the two boundaries are then obtained by making the partial measurements corresponding to observation of the two absorbing states at each time point,

$$p(0,t) = |\psi_R(0,t)|^2 + |\psi_L(0,t)|^2 \quad (14)$$
$$p(4,t) = |\psi_R(4,t)|^2 + |\psi_L(4,t)|^2. \quad (15)$$

So, for instance, the first passage time distributions for a Hadamard walk (see Figure 3) can be easily computed, and are illustrated in Figure 6.

Partially Coherent Quantum Walks

Since in psychology we are rarely confronted with pure systems of any kind, we would like to allow for the possibility that our quantum walks decohere as a result of their interaction with their environment[1]. Decoherence is one pathway from quantum to classical systems so we expect our walks to produce the quantum walk results for low decoherence and the random walk results for high decoherence.

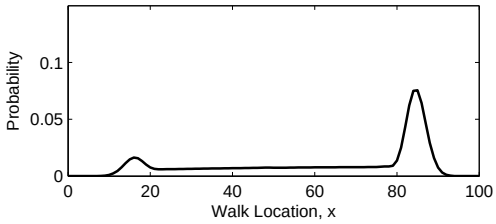

Figure 7: The distribution of a free Hadamard walk (at $t = 50$) with a small amount ($\alpha = 0.1$) of phase damping noise, and a Gaussian distribution over start points (suitably discretized, with mean $x = 50$ and standard deviation 5).

We formulate the partially coherent quantum walk in terms of density matrices $\boldsymbol{\rho}(x,t)$. The density matrix representation for a quantum state is constructed by taking the outer product of the spinor and its adjoint,

$$\boldsymbol{\rho}(x,x',t) = \boldsymbol{\psi}(x,t)\boldsymbol{\psi}^\dagger(x',t). \quad (16)$$

Thus the ij-th cell of the density matrix $\rho_{ij}(x,x',t)$ is simply the product $\psi_i(x,t)\psi_j^*(x,t)$. Accordingly, the main diagonal elements of $\boldsymbol{\rho}$ are real-valued and non-negative, and describe the probabilities (not amplitudes) associated with a particular state. The "correlations" between the states are represented by the off-diagonal elements of the matrix, which are complex-valued.

When adopting the density matrix formulation, we begin by constructing the initial state from the spinor, as follows:

$$\boldsymbol{\rho}(x,x',0) = \boldsymbol{\psi}(x,0)\boldsymbol{\psi}^\dagger(x',0). \quad (17)$$

We then inject noise into the density matrix before applying the time evolution operator $\mathbf{U}$. If we let $\tilde{\boldsymbol{\rho}}(x,x',t)$ denote a noise-corrupted density matrix at time t, then the evolution of the system is described by,

$$\boldsymbol{\rho}(x,x',t+1) = \mathbf{U}\tilde{\boldsymbol{\rho}}(x,x',t)\mathbf{U}^\dagger, \quad (18)$$

and we inject noise once more to arrive at $\tilde{\boldsymbol{\rho}}(x,x',t+1)$, the noise-corrupted density matrix at time $t+1$. In order to include absorbing boundaries at each stage we make partial measurements of the noisy density matrix. In the example with boundaries at $x = 0$ and $x = 4$ to obtain the first passage time probabilities at each time step we measure

$$p(0,t) = \rho_{0,0}(0,0,t) + \rho_{1,1}(0,0,t) \quad (19)$$
$$p(4,t) = \rho_{0,0}(4,4,t) + \rho_{1,1}(4,4,t), \quad (20)$$

noting that in doing so we collapse the first two and last two columns and rows of the density matrix, in analogy with the coherent case state functions.

Choosing a noise model to govern the transition from quantum to classical behavior is not simple. There are a number of plausible candidates for psychological noise processes, each describing a way of calculating $\tilde{\boldsymbol{\rho}}$ from $\boldsymbol{\rho}$ (see Nielsen &

[1]The term "environment" here is intended quite generally - referring to any aspect of the world outside of the decision-system, including other neural systems.

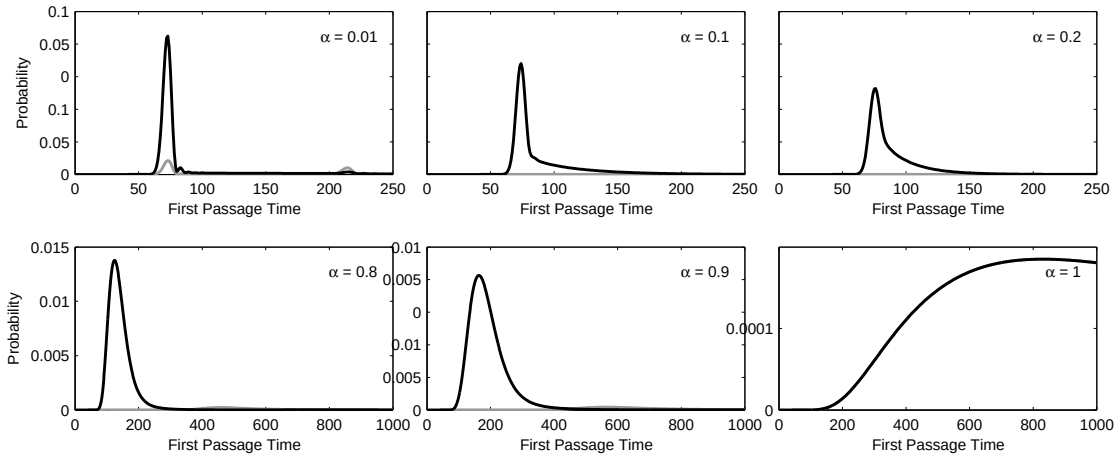

Figure 8: The effect of adding amplitude-damping noise to a Hadamard walk with $a = 100$. From left to right, the top panels show the effect of injecting a small amount of noise into the quantum walk, with α of 0.01, 0.1 and 0.2. The lower panels consider the opposite effect, where the rightmost panel is purely classical ($\alpha = 1$), and the left panels allow very weak quantum effects ($\alpha = 0.8$ and 0.9). The black lines plots the first passage times to the right boundary $x = a$, and the grey line plots hitting times for the left boundary $x = 0$.

Chuang, 2000 for a broader discussion). The basic approach is to apply noise operators $\mathbf{E_0}, \mathbf{E_1}, \ldots, \mathbf{E}_m$ to the density matrix $\boldsymbol{\rho}$, such that

$$\tilde{\boldsymbol{\rho}}(x, x', t) = \sum_{j=0}^{m} \mathbf{E}_j \boldsymbol{\rho}(x, x', t) \mathbf{E}_j^\dagger. \tag{21}$$

It is worth noting the noise and time-evolution operators can be seen as two aspects to a single "noisy evolution". That is, by putting Equations 18 and 21 together, we can directly describe the time evolution of the system using

$$\tilde{\boldsymbol{\rho}}(x, x', t+1) = \mathbf{U} \left(\sum_{j=0}^{m} \mathbf{E}_j \tilde{\boldsymbol{\rho}}(x, x', t) \mathbf{E}_j^\dagger \right) \mathbf{U}^\dagger. \tag{22}$$

For the purposes of the current paper, we briefly mention two simple possibilities. The first, *amplitude damping via spontaneous decay*, arises when a quantum system is coupled with a vacuum The operator formalism for amplitude damping via spontaneous decay is given by

$$\mathbf{E}_0 = \begin{bmatrix} 1 & 0 \\ 0 & \sqrt{1-\alpha} \end{bmatrix}, \qquad \mathbf{E}_1 = \begin{bmatrix} 0 & \sqrt{\alpha} \\ 0 & 0 \end{bmatrix}. \tag{23}$$

The second example we mention is *phase damping* in which

$$\mathbf{E}_0 = \begin{bmatrix} 1 & 0 \\ 0 & \sqrt{1-\alpha} \end{bmatrix}, \qquad \mathbf{E}_1 = \begin{bmatrix} 0 & 0 \\ 0 & \sqrt{\alpha} \end{bmatrix}. \tag{24}$$

However, there it is straightforward to modify the approach to accommodate other noise models, such as generalized amplitude damping or depolarization.

As discussed previously, our primary aim in this paper is to extend the psychological theory developed by Busemeyer et al. (2006), and illustrate how injecting noise into the walk gives rise to partially-coherent walks that preserve the desirable characteristics of their classical counterparts, while retaining some of the interesting properties of the pure quantum walks. While the psychological theory is a long way from being fully developed, it is worth discussing the kinds of empirical data patterns that the partially-coherent walks are able to capture. To illustrate this, Figure 8 show the first passage time distributions for an amplitude-damped Hadamard walk at several different levels of noise. From a psychological perspective, two relevant effects are illustrated. Firstly, as is clear from the top panel, only very small amounts of noise are required to smooth out the interference patterns in Figure 6 (they are gone even at $\alpha = 0.01$); some "quantum tunnelling" effects are still observable at this level (i.e., the second mode at about $t = 200$), but those too are gone once α reaches 0.1. In contrast, the lower panels show the converse effect: allowing even a modest degree of coherence to persist in the state (e.g., with $\alpha = .9$) produces an enormous speed up to the decision times. However, some refinement is clearly required: for instance, this particular noise model suppresses the drift to the left boundary, so the "error" rate remains near zero across most values of α.

Discussion

Sequential sampling models are at present the best formal framework available for modeling accuracy, latency, and confidence in simple decisions. In Gigerenzer and Todd's (1999) terms, they make reasonable assumptions about how people gather evidence (*information search*), when they stop (*termination rules*), and what decision is then made (*decision rule*). However, while this framework places some constraints on what kinds of models are admissable, it still allows considerable variation in the low-level details; some evidence-accrual models are continuous (Ratcliff, 1978) and others discrete (Smith & van Zandt, 2000). Variation in termination rules also exists, with a distinction made between accumulator (Vickers, 1979) and random walk models.

In their recent paper (Busemeyer et al., 2006) argue that, in addition to these existing issues, psychological evidence-accrual based on quantum walks needs to be considered alongside its classical counterpart. One method to accommodate this issue is to consider more general models that trace out a path from the purely quantum to purely classical, in

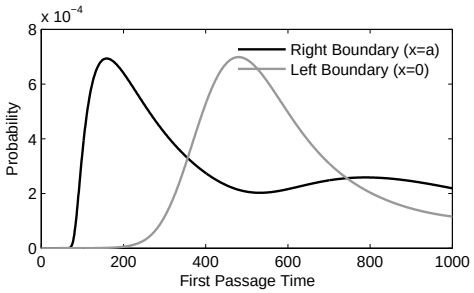

Figure 9: First passage times to the two boundaries (with $a = 100$) for an amplitude-damped ($\alpha = 0.2$) walk with $k = 0$, $r = -i/\sqrt{2}$ and $s = 1/\sqrt{2}$.

much the same way that competitive accumulators can move from random walk to accumulator behavior (Usher & McClelland, 2001). Such models would exhibit a broad spectrum of behaviors that correspond to quantum systems of varying degrees of coherence.

In this paper we have developed exactly such a class of models, inducing partial decoherence by injecting noise into the walk. Of particular note is that partially-coherent quantum systems produce first passage time distributions that often have shapes similar to classical walks (smoothing over the jagged distributions produced by the pure system), but predict much faster response times. This indicates that inference from human reaction data for or against the possibility of quantum or quantum-like processes giving rise to human behavior is more subtle than previously envisaged. In part, this subtlty arises from the inherent complexity associated with inverting the reaction time profiles to obtain the underlying evidence gathering processes (the well-known model mimicry problem; e.g., Ratcliff & Smith, 2004). The bimodal shapes of the noisy Hadamard walks, for example, are quite different from the unimodal shape of the Bernoulli walk, yet the two often produce similarly shaped first-passage time distributions.

An important point worth noting, however, is that a number of the shapes that these models can produce appear to be quite distinct from the classical distributions, potentially allowing explicit experimental tests to be developed. To give a simple example, Figure 9 provides a case in which amplitude-damping noise is added to a (non-Hadamard) walk that is normally symmetric. However, in this case the noise breaks the symmetry of the walk, and creates quite unusual-looking first-passage time distributions. We suggest that the ability to extract this kind of first passage time distribution from a partially-coherent quantum walk is precisely what is needed, as a prerequisite for constructing genuine experimental tests of the hypothesis that the simple decisions make use of quantum mechanics.

One final issue bears mentioning: besides the potential value in enabling research into the extent to which the mind satisfies quantum mechanical principles, partially-coherent walks tie into a long-standing issue in response time modeling, namely the extent to which evidence accrues serially or in parallel (see, e.g., Townsend & Ashby, 1983). In quantum walks evidence accrual occurs in parallel, whereas classical walks are serial. One interesting line of work would be to make explicit connections to existing serial-parallel discussions.

Acknowledgements. Portions of this work were presented at the second Quantum Interaction symposium in Oxford, March 2008. DJN was supported by an Australian Research Fellowship (ARC grant DP0773794).

References

Aharonov, Y., Davidovich, L., & Zagury, N. (1993). Quantum random walks. *Phys. Rev. A.*, *48*, 1687-1690.

Busemeyer, J. R., Wang, Z., & Townsend, J. T. (2006). Quantum dynamics of human decision-making. *Journal of Mathematical Psychology*, *50*, 220-241.

Diederich, A., & Busemeyer, J. (2003). Simple matrix methods for analyzing diffusion models of choice probability, choice response time and simple response time. *Journal of Mathematical Psychology*, *47*, 304-322.

Feller, W. (1968). *An introduction to probability theory and its applications*. New York: Wiley.

Fuss, I., White, L. B., Sherman, P., & Naguleswaran, S. (2007). Analytic views of quantum walks. *Proc. Of SPIE, Noise and Fluctuations in Photonics, Quantum Optics and Communications, 6603*.

Gigerenzer, G., & Todd, P. M. (1999). *Simple heuristics that make us smart*. Oxford: Oxford University Press.

Grover, L. K. (1997). Quantum mechanics helps in searching for a needle in a haystack. *Phys. Rev. Lett.*, *79*, 325.

Hameroff, S. R. (2007). The brain is both neurocomputer and quantum computer. *Cognitive Science*, *31*, 1035-1045.

Litt, A., Eliasmith, C., Kroon, F. W., Weinstein, S., & Thagard, P. (2006). Is the brain a quantum computer? *Cognitive Science*, *30*, 593-603.

Luce, R. D. (1986). *Response times: Their role in inferring elementary mental organization*. New York, NY: Oxford University Press.

Meyer, D. A. (1996). From quantum cellular automata to quantum lattice gases. *Journal of Statistical Physics*, *85*, 551-574.

Nielsen, M. A., & Chuang, I. L. (2000). *Quantum computation and quantum information*. Cambridge, UK: Cambridge University Press.

Penrose, R. (1989). *The emperor's new mind: Concerning computers, minds and the laws of physics*. Oxford Unversity Press.

Ratcliff, R. (1978). A theory of memory retrieval. *Psychological Review*, *85*, 59-108.

Ratcliff, R., & Smith, P. L. (2004). A comparison of sequential sampling models for two-choice reaction time. *Psychological Review*, *111*, 333-367.

Shor, P. W. (1994). Algorithms for quantum computation: discrete logarithms and factoring. In S. Goldwasser (Ed.), *Proceedings of the 35th annual symposium on foundations of computer science* (p. 124-134). Los Alamitos, CA: IEEE Press.

Shor, P. W. (1997). Polynomial time algorithms for prime factorisation and discrete logarithms on a quantum computer. *SIAM J. Comp.*, *26*, 1484-1509.

Smith, P. L. (2000). Stochastic dynamic models of response times and accuracy: A foundational primer. *Journal of Mathematical Psychology*, *44*, 408-463.

Smith, P. L., & van Zandt, T. (2000). Time dependent poisson counter models of response latency in simple judgment. *British Journal of Mathematical and Statistical Psychology*, *53*, 293-315.

Stone, M. (1960). Models for choice reaction time. *Psychometrika*, *25*, 251-260.

Townsend, J. T., & Ashby, F. G. (1983). *Stochastic modeling of elementary psychological processes*. Cambridge, UK: Cambridge University Press.

Usher, M., & McClelland, J. L. (2001). The time course of perceptual choice: The leaky, competing accumulator model. *Psychological Review*, *108*, 550-492.

Vickers, D. (1979). *Decision processes in visual perception*. New York, NY: Academic Press.

Wald, A. (1947). *Sequential analysis*. New York: Wiley.